

SPATIAL AND TEMPORAL VARIABILITY OF LONGSHORE TRANSPORT ALONG GOLD COAST, AUSTRALIA

Kristen D. Splinter¹, Aliasghar Golshani¹, Greg Stuart^{1,2}, and Rodger Tomlinson¹

Spatial and temporal variability of longshore transport potential for a 35-km stretch of sandy coastline on the east coast of Australia is examined using a 25-year data set. Six-hourly offshore wave data is binned into yearly wave classes using a global k -means algorithm that accounts for wave height, period, and direction simultaneously. Wave class estimates are shoaled into the nearshore using MIKE 21 Spectral Wave (SW) model. Longshore transport is calculated using the formulas of Kamphuis (1991; 2002) and Bayram et al. (2007) and show good agreement with previously published estimates for the Gold Coast, suggesting the wave classification scheme sufficiently represents the variability in yearly wave data. Results show large temporal and spatial variability of transport potential along the coastline. Spatial variation is attributed to shoreline orientation and wave exposure, while temporal variability is significantly correlated with variations in the Southern Oscillation Index.

Keywords: sediment transport; longshore transport; shoreline change; climate variability; Gold Coast, Australia.

Introduction

The majority of the world's coastlines are characterized by sandy shorelines that display large temporal and spatial variability due to changing wave climate and sediment supply. Both the onshore-offshore transport of sand, as well as gradients in the longshore transport of sand can influence the temporal variability of the shoreline. As waves break, they release their energy into the water column via radiation stress gradients that in turn drive currents. While cross-shore transport is linked to variations in wave height and the contributions from cross-shore currents and wave breaking processes, longshore transport is a result of oblique wave action and longshore currents. The sand grains are mobilized by the short-wave orbital velocities and turbulent energy of the breaking waves and subsequently carried along the coast by these currents. When assessing long term shoreline variability associated with sea level rise and climate variability, Cowell et al. (1995) showed that a 1% deficit in longshore transport sand supply could have the same impact as 0.5 m sea level rise in terms of shoreline retreat and is therefore an important parameter that needs to be addressed in any future climate change scenarios.

In this paper, we focus on the temporal and spatial variability of longshore transport along a 35-km stretch of coastline on the east coast of Australia. It has long been assumed that the net longshore transport in the Gold Coast region is approximately 500,000 m³/yr to the north due to the predominant south-easterly swell wave climate. However, several studies (DHL 1992; Patterson 2007) have shown that longshore transport can vary considerably along the coast and from year to year due to the location, frequency and intensity of storms with respect to the coastline. The southern end of the Gold Coast is largely protected by Point Danger against strong southerly swell, while the northern end of the coast is exposed to a much larger wave climate, suggesting longshore gradients in transport should be expected along the coast. Recent studies have linked beach rotation and shoreline realignment to wave climate variability associated with larger scale climate variability (e.g. Ranasinghe et al. (2004) and Goodwin et al. (2006)). These temporal variations, which may be linked to climate indices such as the Southern Oscillation Index (SOI) and the Inter-decadal Pacific Oscillation (IPO), can have large implications for coastal management and engineering works and need to be addressed.

Here we develop a method to classify the yearly offshore wave climate into distinct bins, or classes, describing the various forcing mechanisms. Offshore waves are then shoaled and refracted into the nearshore using the spectral wave model, MIKE 21 SW. Breaking conditions at eight locations along the Gold Coast are used to estimate longshore transport potential and describe the spatial and temporal variability of longshore transport potential with respect to climate variability.

¹ Griffith Centre for Coastal Management, Griffith University, Gold Coast Campus, Parklands Dr., Southport, QLD, 4216, AU

² DHI Group, Suite 1801, Level 8, 56 Scarborough Street, Southport, QLD, 4215, AU

Study Area

Geography

The Gold Coast region is situated at the south-eastern tip of Queensland, Australia (Figure 1). The 35-km coastline has a general crenulate shape, extending from the Tweed River entrance along the New South Wales border at the southern end to the mouth of the Nerang River at the northern tip. Both rivers, along with two minor creeks, Currumbin and Tallebudgera, are considered sinks and do not supply sand to the nearshore system. However, dredging of Currumbin and Tallebudgera creeks provide minor amounts of sand to adjacent beaches. Point Danger, Currumbin Rock, and Burleigh Headland act as natural barriers to longshore transport. The nearshore morphology is described as an energetic intermediate beach (Wright and Short 1984) double-barred system (van Enckevort et al. 2004). Under high wave conditions, the bars move offshore and ‘reset’, becoming longshore uniform, while under the influence of milder waves, the bars move back onshore and the morphology is characteristically rip-dominated (Turner et al. 2007). Beach sands are classified as fine sand-sized grains ($0.2 \text{ mm} < d_{50} < 0.3 \text{ mm}$).

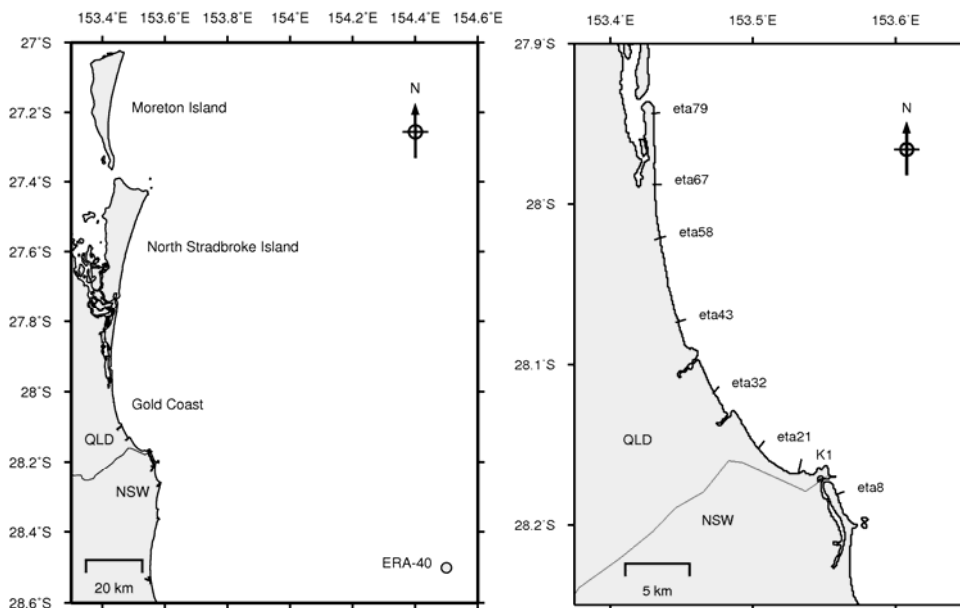


Figure 1. (Left) Map of Southern Queensland – Northern New South Wales Coast and location of study site, Gold Coast. ERA-40 grid point where wave data is extracted from is given at bottom right. (Right) Detailed map of Gold Coast region with survey locations marked.

Wave Climate

The roughly east-facing coast is exposed to energetic wave conditions throughout the year. The wave climatology of the Gold Coast can be subdivided into four main categories: Ground swell (GS), wind swell or local wind seas (WS), East Coast Lows (ECL), and tropical cyclones (TC). Ground swell is the dominant offshore wave climate and is typically generated in the mid-latitudes and Southern Ocean. These waves occur year-round and are characterized by long periods and low wave heights with a south-easterly to southerly direction. Wind seas are locally generated, short period waves and wave height and direction can vary depending on the strength, duration, and direction of wind. These conditions are common in the summer months when daytime heating over the mainland causes strong onshore breezes from late morning to early evening. The two most energetic types of waves that affect the Gold Coast are East Coast Lows and tropical cyclones. East Coast Lows are intense low pressure systems typically generated off the south-east tip of Australia in the Tasman Sea. These typically occur in the austral autumn to winter months (April – August), with June being the most common. These storms can last several days and bring large waves, high winds, and rains to the coast. Tropical cyclones are typically generated in Northern Queensland in the Coral Sea and rarely propagate as far south as Southern Queensland. However, their effects are still present as a northerly swell influencing the coast during the late austral summer to autumn (January – March). The predominance of south-easterly waves results in a net longshore transport to the north.

Engineering Works

The Gold Coast region is highly engineered (Colleter et al. 2001; D'Agata and Tomlinson 2001; Delft Hydraulics Laboratory 1970; Delft Hydraulics Laboratory 1992). Training walls at the Nerang and Tweed River entrances were built to maintain safe channel navigation. Due to the disruption of longshore transport at these locations, sand-by passing systems have been implemented in an effort to maintain the natural rate of longshore transport. Pumping rates vary between 400,000 m³/yr and 800,000 m³/yr depending on the wave climate. Jetties at Currumbin and Tallebudgera Creeks, as well as, groynes at Coolangatta, Kirra, and Palm Beach alter the local longshore transport and the shoreline. At the northern end of the Gold Coast an artificial reef located offshore of Narrowneck is used for shoreline protection (Turner et al. 1999). Lastly, a boulder wall running parallel to the coastline exists along much of the coast as a last line of defense against storm induced erosion.

Methods

Offshore Wave Data

Offshore wave characteristics are estimated every 6 hours using global wind-wave models such as the European Centre for Medium-Range Weather Forecasts (ECMWF) 40 year wave re-analysis (ERA-40) or the National Oceanographic and Atmospheric Administration (NOAA) WaveWatch III (WWIII). We have chosen to use the ERA-40 wave data as it is the longest, directional wave record available in this area. Caires and Sterl (2005) noted that the original ERA-40 model (1958 – 2001) under-estimated large waves compared to measured data and applied a correction factor to the ERA-40 wave heights resulting in a corrected data set known as the C-ERA-40. Here we use the C-ERA-40 (1958 - 2001) (Caires and Sterl 2005) and ERA-Interim (1989 - present) data sets extracted from grid point coordinates (154.5,-28.5) located roughly 122 km south east from the Gold Coast Seaway (Figure 1 left). To combine data sets, over-lapping time series between the initiation of the ERA-Interim reanalysis and the C-ERA-40 data sets (number of comparison points=18,992) were used to determine a non-linear correction factor for the ERA-Interim wave heights using a Generalized Additive Model (GAM) technique (Figure 2).

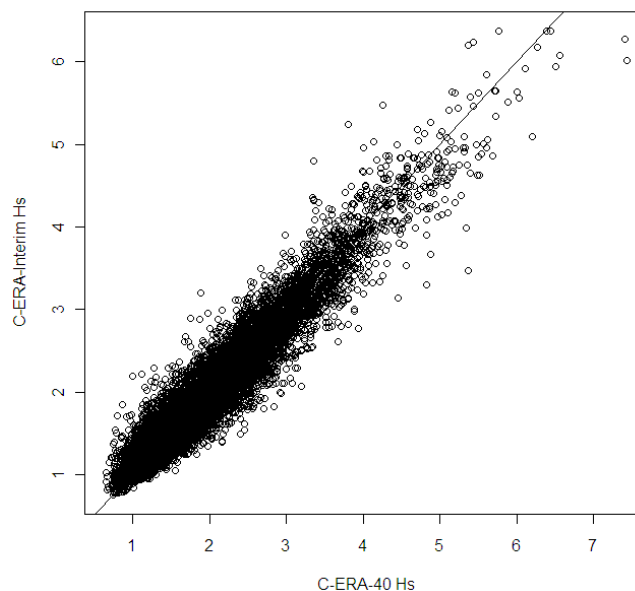


Figure 2. Comparison of C-ERA-40 H_s and C-ERA-Interim H_s based on nonlinear correction. $R^2=0.92$. Solid line represents 1:1.

Propagating the 6-hourly wave values to nearshore conditions may provide increased accuracy in sediment transport results, but at a computational cost that is prohibitive for long term analysis. In this respect, classifications, or groups can be identified to represent the full spectrum of waves for a given time period. Each representative wave condition can then be shoaled and refracted into the nearshore to determine breaking conditions, therefore reducing the number of computations drastically.

Wave Classification

The classification scheme is based on the data clustering methodology of Bagirov (2008). The process is iterative, such that a minimum tolerance for changes in cluster centres, x^j , rather than the number of clusters, k , is defined by the user. In this respect, the spread of the data determines the number of clusters. The distance, or function, to be minimized is:

$$\psi_k(X, w) = \frac{1}{m} \sum_{i=1}^m \sum_{j=1}^k w_{ij} \|x^j - a^i\|^2, \quad (1)$$

where

$$X = (x^1, \dots, x^k) \in \mathbb{R}^{n \times k} \quad (2)$$

is the vector of all cluster centers, x^j , m is the total number of data points considered in \mathbb{R}^n , the real-valued n -dimensional space, w_{ij} is a weighting function that is equal to 1 if data point, a^i , is within cluster j , and 0 if it lies outside. We represent each data point by the wave height, H , wave period, T , and wave direction, θ , based on the work of Butel et al. (2002). Bertin et al. (2008) suggest that in order to capture extreme events, H^2 , rather than H , should be used, such that we express the generalized distance equation (Dagnelie 1975) as:

$$\|x^j - a^i\| = \sqrt{\frac{(H_j^2 - H_i^2)^2}{\sigma_{H^2}^2} + \frac{(T_j - T_i)^2}{\sigma_T^2} + \frac{(\theta_j - \theta_i)^2}{\sigma_\theta^2}}, \quad (3)$$

where σ implies the standard deviation of the associated variable.

Nearshore Wave Conditions

Significant wave height, H_s , peak wave period, T_p , and mean wave direction, θ , are used as offshore boundary conditions for the spectral wave model, MIKE 21 SW. The MIKE 21 SW model is one of the state-of-the-art numerical modeling tools for studying spectral wind-waves in the nearshore. The model uses a flexible mesh grid, allowing for coarse resolution offshore and fine resolution near the shoreline and around complex bathymetry, making it applicable for simultaneous wave analysis at both regional and local scales. The model can run in both stationary and non-stationary mode. The governing equations account for wind-generated wave growth, non-linear wave-wave interaction, refraction and shoaling due to depth variations, wave-current interaction and the effect of time-varying water depth, as well as wave dissipation due to white-capping, bottom friction, and depth-induced wave breaking.

In this study, each wave class is run in stationary mode and nearshore wave heights prior to breaking are extracted along the eight predefined transect lines. The bathymetry file is constructed from available yearly surveys obtained from the Gold Coast City Council and the Electronic Chart Database CM-93 Edition 3.0. A two-dimensional (flexi-mesh and depth-averaged) grid represents the study area of approximately 30,000 km² with 48,802 elements and 24,827 nodes. The resolution of elements progressively increases shoreward from 5 km for the offshore mesh to 50 m in 10 m depth of water. Open boundaries are used on the eastern offshore boundary and along the southern boundary. The northern boundary is partially open and partially closed and the western land boundary is regarded as a closed boundary.

Longshore Sediment Transport

Longshore transport is a direct result of sediment properties and the longshore current generated from oblique wave incidence. Wave height, period, and wave angle all contribute to the longshore current through the transfer of momentum from the breaking waves to the water column. Eight sites along the Gold Coast from Letitia Spit (at the south) to The Spit (at the north) are used to analyze spatial gradients due to varying local wave climate, beach slope, and shoreline orientation (Figure 1 right). Modeled wave heights along the pre-defined survey transects are used to estimate the location of breaking and extract breaking wave height, H_b , and breaking wave angle, θ_b . Longshore drift at each site is computed using the formulation of Kamphuis (1991; 2002):

$$Q(m^3/s) = \frac{0.0013\rho_w}{(\rho_s - \rho_w)(1-p)} \frac{H_b^3}{T_p} \left(\frac{H_b}{L_o}\right)^{-1.25} \tan \alpha_b^{0.75} \left(\frac{H_b}{d_{50}}\right)^{0.25} \sin^{0.6}(2\theta_b), \quad (4)$$

where ρ_w is the density of water (1024 kg/m³), ρ_s is the sediment density (2650 kg/m³), p is the sediment porosity (0.04), L_o is the deep water wave length, and d_{50} , is the mean sediment diameter (0.22 mm). The mean profile slope between the shoreline and the 5 m contour is represented by $\tan \alpha_b$ and accounts for both spatial and temporal changes to the overall beach profiles along the coast. A second equation, described in Bayram et al. (2007), was shown to have better agreement over a wide range of field and lab conditions and is therefore used to compare against equation (4). Their equation for sediment transport is:

$$Q(m^3/s) = \frac{\varepsilon}{(\rho_s - \rho_w)(1-p)gw_s} F\bar{V}, \quad (5)$$

where g is the acceleration due to gravity (9.81 m/s²), w_s is the sediment fall velocity, ε is an efficiency factor, F , is the cross-shore component of wave energy flux, and \bar{V} is the mean longshore current. Bayram et al. (2007) assume sediment is brought into (and held in) suspension by breaking waves, defined here by an efficiency term, ε :

$$\varepsilon = \left(9.0 + 4.0 \frac{H_b}{w_s T_p}\right) \cdot 10^{-5}, \quad (6)$$

and is a function of the non-dimensional fall velocity. The cross-shore wave energy flux for oblique waves, F , is defined as:

$$F = E_b C_{gb} \cos \theta_b = \frac{1}{8} \rho_w g H_b^2 \sqrt{g \left(\frac{H_b}{\gamma_b}\right)} \cos \theta_b, \quad (7)$$

where E_b is the breaking wave energy, C_{gb} , is the group velocity measured at breaking, and γ_b is the breaker parameter (0.78). Although the mean current can include components due to tides, winds, waves, or other geostrophic effects, here we consider only the component due to oblique wave action assuming an equilibrium beach profile:

$$\bar{V} = \frac{5}{32} \frac{\pi \gamma_b \sqrt{g}}{c_f} A^{3/2} \sin \theta_b, \quad (8)$$

where A is the shape parameter (van Rijn 1993) and c_f is a friction coefficient (0.005).

Results

Waves

Offshore wave classes were calculated for the 25 year period (1985 - 2009). A significant number of classes describe the ground swell signal from the south east. For 2008 (Table 1), 67% of the data was classified as ground swell, 27% was wind sea, and the remaining 11% was due to storm activity. The wave classes for 2008 are shown in Figure 3.

| Table 1. Offshore ERA-40 wave classification breakdown for 2008. Wave direction is given in degrees North based on nautical convention. | | | | | |
|---|--------|--------------------|--------------------|--------|---|
| Class | % time | H _s (m) | T _p (s) | θ (°N) | Comments (GS = ground swell, WS = wind swell) |
| 1 | 23 | 1.76 | 8.76 | 135 | Year round GS |
| 2 | 20 | 2.18 | 8.87 | 141 | Year round GS |
| 3 | 13 | 1.32 | 8.49 | 148 | Winter GS |
| 4 | 11 | 2.80 | 9.05 | 150 | Fall GS |
| 5 | 11 | 1.32 | 7.45 | 95 | Summer WS |
| 6 | 7 | 1.41 | 6.54 | 31 | Spring – summer WS |
| 7 | 5 | 3.61 | 9.37 | 152 | ECL and mid-lat storms |
| 8 | 5 | 1.84 | 6.80 | 26 | Spring WS |
| 9 | 4 | 1.72 | 6.68 | 298 | Summer WS, offshore direction |
| 10 | 2 | 4.86 | 10.32 | 160 | ECL and mid-latitude storms |

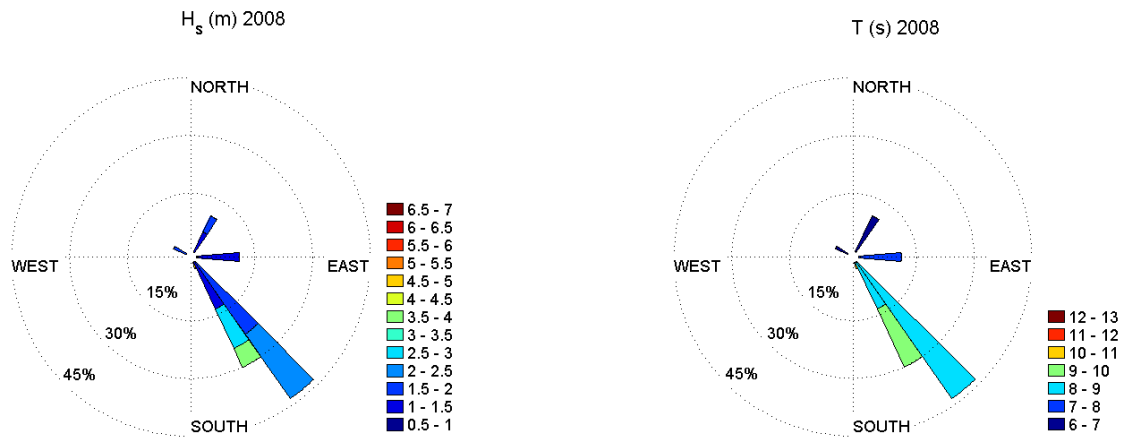


Figure 3. Example wave classification for 2008. (Left) Wave height variation as a function of direction and percentage of occurrence. (Right) Corresponding analysis for wave period. Colors represent the magnitude of wave height and period.

Due to the orientation of the coast and the dominant SE wave climate, considerable wave shadowing in the lee of Point Danger (just north of ETA 08) occurs at the southern end of the study area (sites K1 – ETA 32) (Figure 4). Average breaking wave heights at the more exposed ends of the coast (ETA 08 and ETA 79) were approximately 1.5 m, while the most sheltered site, Kirra (K1), had a mean wave height of 0.9 m. When we consider transport as a nonlinear function of wave height, this has considerable impact on the total transport along the coast.

Longshore Transport

Examining the net transport estimates for 2008 (Figure 5), ground swell wave classes (1 - 4), representing 67% of the data account for roughly 62% of the gross transport. In comparison, the storm classes (7 and 10), representing just 7% of the wave data account for roughly 23% of the gross transport, with the remaining 15% attributed to the wind sea events. While transport contribution related to wind and ground swell generated currents are roughly equivalent to their percent occurrences, storm events play a disproportionate role on the yearly transport estimates. This suggests that if the number of storms varies considerably between years, we would expect to see much larger variations in transport as well.

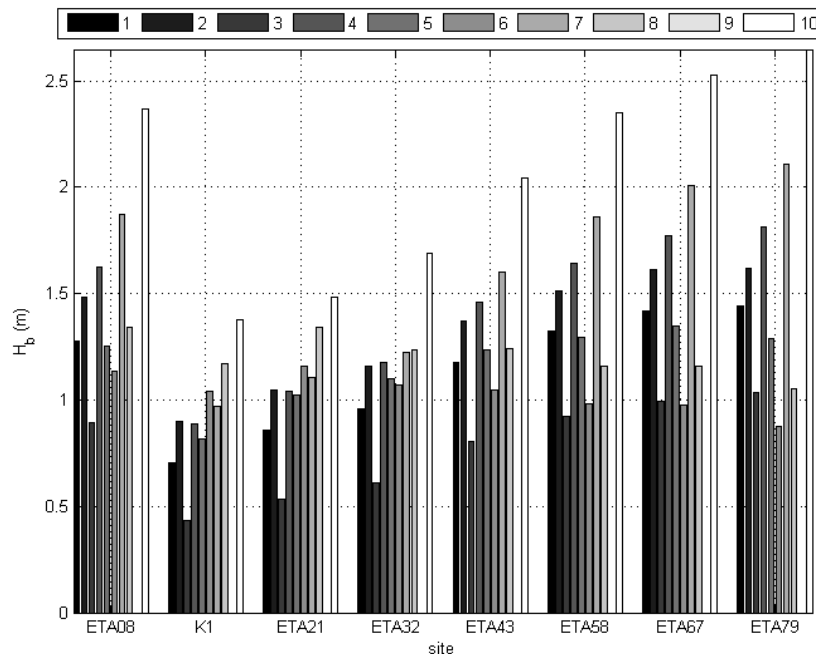


Figure 4. Breaking wave statistics at each site for 2008. Each color bar represents a different class as defined in Table 1. Note class 9 is omitted as it is offshore directed.

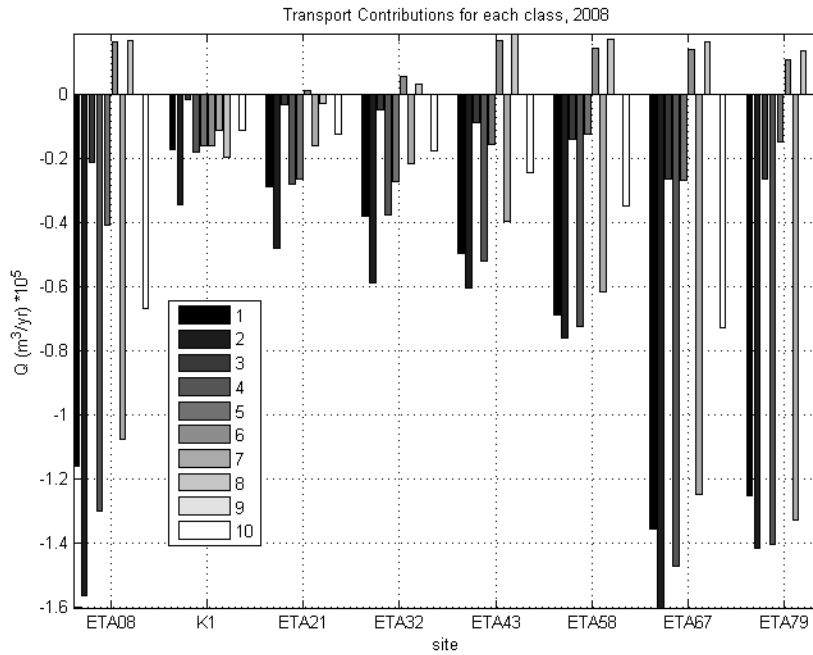


Figure 5. Net transport by class for 2008 using Bayram et al. (2007).

Considerable variation between the transport estimates for the two transport equations exist (Figure 6). Results using the Bayram et al. (2007) equation show better agreement with previously published results for longshore transport along the Gold Coast at the more exposed sites (Patterson 2007). Bayram et al. (2007) noted in their analysis that the Kamphuis equation over-predicted transport under lower energy conditions. Since ground swell events make up the majority of the yearly wave climate along the Gold Coast their finding is in qualitative agreement with our results here. However, due to the sensitivity of each equation with respect to input parameters, such as beach slope, sediment grain size, and beach orientation, we must consider both results to be reasonable estimates of longshore transport.

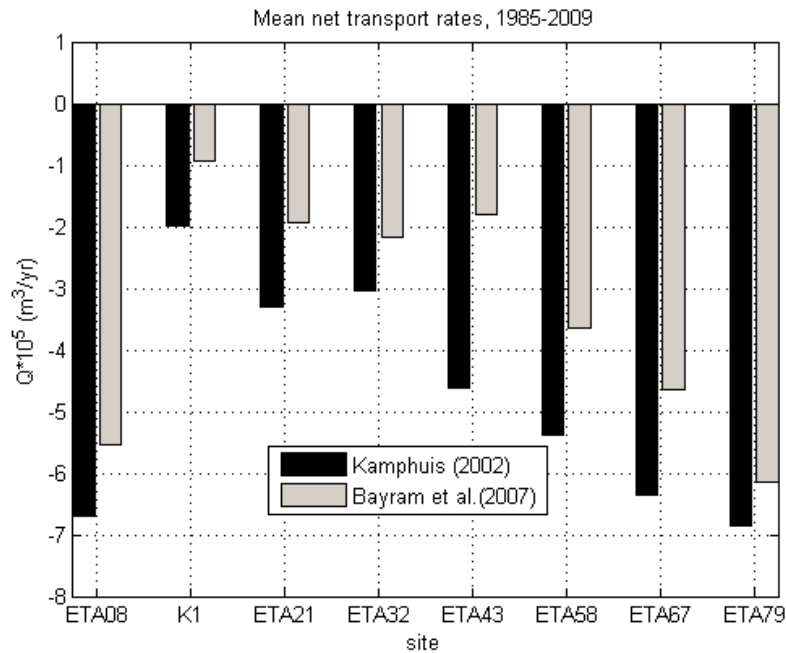


Figure 6. Mean net transport rates for 1985-2009.

Spatial and Temporal Variability

Mean southerly, Q_S , northerly, Q_N , gross, Q_{GROSS} , and net, Q_{NET} , transport, as well as, the standard deviation, σ_Q , in net transport for each site is given in Table 2. Northerly transport is an order of magnitude greater than the southerly component, resulting in a strong net northerly drift. At the southern sites (K1 – ETA 32) the orientation of the coast results in minimal southerly transport. There is a general increasing trend of northerly longshore transport with increasing northerly location. The results given here are in good agreement with Patterson (2007) for Narrowneck and The Spit (ETA 67 and 79, respectively). Longshore transport estimates for Burleigh Beach are lower in our analysis, but as the exact ETA line was not given in Patterson (2007), direct comparison is difficult. Transport rates at ETA 08 and 79 are similar due to their comparable exposure to both southerly and northerly waves.

| Site | $Q_S(m^3/yr) * 10^9$ | $Q_N(m^3/yr) * 10^9$ | $Q_{GROSS}(m^3/yr) * 10^9$ | $Q_{NET}(m^3/yr) * 10^9$ | $\sigma_Q(m^3/yr) * 10^9$ |
|--------|----------------------|----------------------|----------------------------|--------------------------|---------------------------|
| ETA 08 | 0.13 | -6.25 | 6.38 | -6.12 | 1.88 |
| K1 | 0.00 | -1.45 | 1.45 | -1.45 | 0.77 |
| ETA 21 | 0.01 | -2.62 | 2.63 | -2.61 | 1.16 |
| ETA 32 | 0.03 | -2.63 | 2.66 | -2.61 | 1.00 |
| ETA 43 | 0.26 | -3.46 | 3.72 | -3.20 | 2.73 |
| ETA 58 | 0.13 | -4.64 | 4.77 | -4.52 | 1.28 |
| ETA 67 | 0.19 | -5.69 | 5.87 | -5.50 | 1.67 |
| ETA 79 | 0.19 | -6.70 | 6.89 | -6.51 | 2.13 |

The standard deviation of transport indicates there is considerable temporal variability at several locations compared to the net transport (e.g. Burleigh Beach (ETA 43)). Yearly estimates of longshore transport at four sites are shown in Figure 7. While all sites show inter-annual variability, the more exposed areas of the coast (i.e. ETA 43 - ETA 79) show a clear cyclic pattern. Although Kirra displays a cyclic nature, it also shows an increasing trend in transport. The reasons for this increase in transport may be a result of the implementation of the sand by-passing system and realignment of the shoreline over time or to larger-scale shifts in wave climate and is an area of future research.

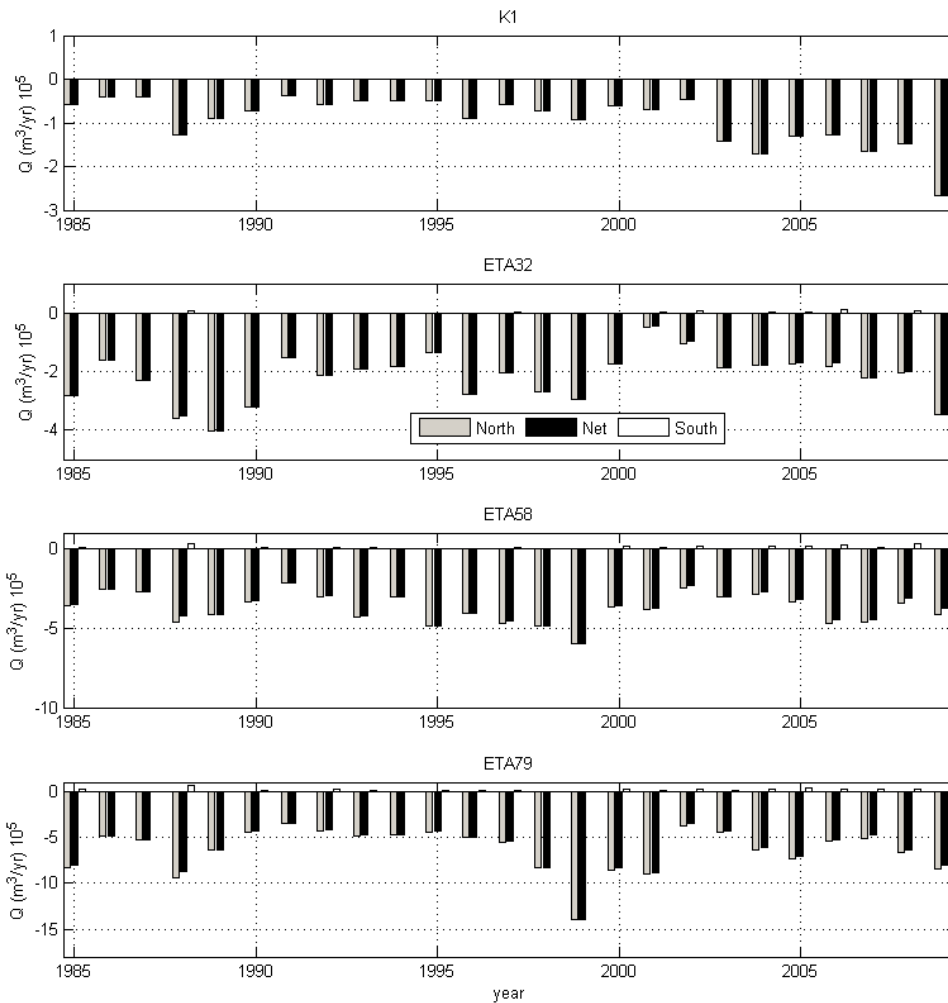


Figure 7. Temporal variability of longshore transport at 4 sites (top to bottom): Kirra, Palm Beach, Broadbeach, and The Spit.

Simple lagged cross-correlations between climate indices (SOI and IPO) and longshore transport showed significant relationships at the expected timescales. All eight sites had significant correlations between yearly net longshore transport and the yearly average SOI index at the 0 and 7-12 year lag. Several sites also showed significant correlations between transport and the IPO at timescales of 10-20 years, however, this relation is less clear due to the short record length and further analysis is required to make any robust conclusion to the link between IPO forcing and longshore transport rates. For ETA 08, significant correlations against the SOI index were seen at 0 and ~10-11 yr lag and ~16 yr lag for the IPO (Figure 8 top).

A simple linear regression model at 0 lag was used to test the dependencies of longshore transport on both the yearly average SOI and IPO indices:

$$Q_{est} = \beta_0 + \beta_1 SOI + \beta_2 IPO , \tag{9}$$

where β represents the best-fit regression coefficients. The model was able to reproduce the temporal variability with significant skill (95% level) at 6 of the 8 sites. For ETA08, the linear regression model for transport using yearly-averaged climate indices showed good agreement with model results (Figure 8, bottom, $R^2=0.47$), with the majority of the temporal variability being attributed to variations in the SOI index.

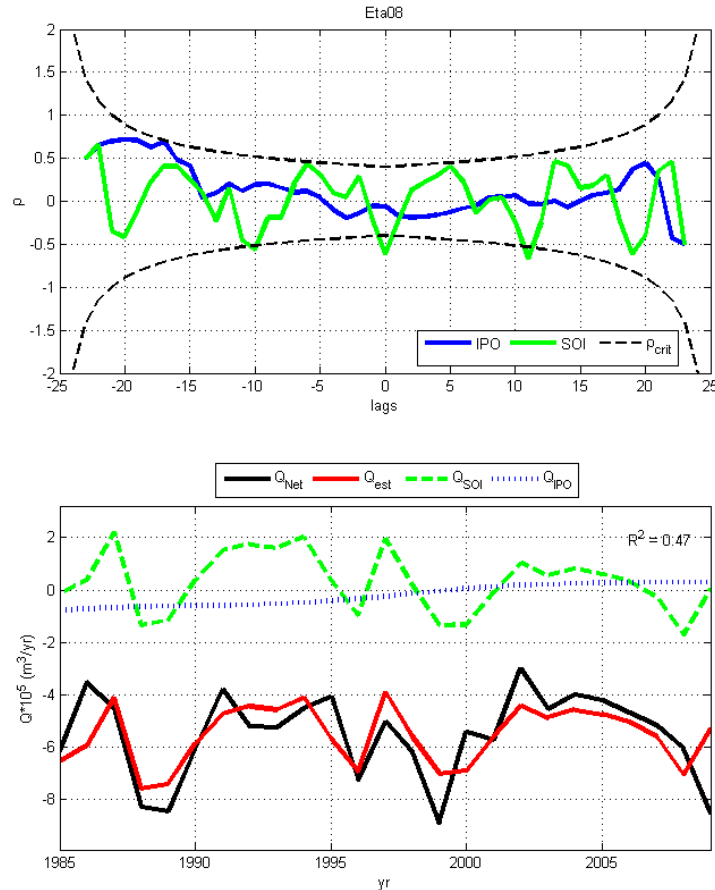


Figure 8. (Top) Example lag-correlation results for ETA 08 against the SOI and IPO index. ρ_{crit} is the correlation cutoff defining critical skill at the 95% level. (Bottom) Longshore transport estimate using simple linear regression of SOI and IPO at 0 lags. $\beta_0 = -5.640894 \cdot 10^5$, $\beta_1 = -0.374767 \cdot 10^5$, $\beta_2 = -0.169351 \cdot 10^5$ m³/yr.

Conclusions

A new wave classification scheme based on a modified global k -means technique was developed to estimate yearly wave climates using the three main wave parameters (H_s , T_p , θ) simultaneously. The number of classes in a given year was determined by the spread in the data and a user defined tolerance. Results were then analyzed and classified as one of the four main types of wave events that occur along South-East Australia. The dominant wave class is long period ground swell generated in the Southern Ocean and occurs year round. Wind seas tend to occur in the austral spring to early fall and characteristically have shorter periods and smaller wave heights. Storm events, such as East Coast Lows generated in the Tasman Sea and tropical cyclones generated in the Coral Sea are the most extreme events and occur in late austral summer to fall.

Longshore transport estimates using the yearly wave classes showed good agreement with previous studies and suggests this simplified approach can be used as an alternative to full temporal analysis, therefore significantly reducing computation cost without a loss in accuracy beyond that inherently presumed in the equations. Results showed significant spatial and temporal variability of longshore transport along this stretch of coastline. Spatial variations were attributed to wave shadowing of the southern beaches by Point Danger, while temporal variations were significantly correlated to variations in the Southern Oscillation Index and the associated variability in wave climate.

Acknowledgments

The authors would like to thank A. Sterl (KNMI) for providing the C-ERA40 data set as well as R. Butel for his insight into the classification scheme. The IPO data set was provided by C. Folland (UKMet). Survey data was provided by Michael Walsh at Gold Coast City Council. Funding for this research was provided by the Queensland Smart State Innovation Fund and Griffith University.

References

- Bagirov, A. M. (2008). "Modified global k-means algorithm for minimum sum-of-squares clustering problems." *Pattern Recognition*, 41, 3192-3199
- Bayram, A., Larson, M., and Hanson, H. (2007). "A new formula for the total longshore transport sediment transport rate." *Coastal Engineering*, 54, 700-710
- Bertin, X., Castelle, B., Chaumillon, E., Butel, R., and Quique, R. (2008). "Longshore transport estimation and inter-annual variability at a high-energy dissipative beach: St. Trojan beach, SW Oleron Island, France." *Continental Shelf Research*, 28, 1316-1332.10.1016/j.csr.2008.03.005
- Butel, R., Dupuis, H., and Bonneton, P. "Spatial Variability of Wave Conditions on the French Atlantic Coast using In-Situ Data." *7th International Coastal Symposium*, Northern Ireland, 96-108.
- Caires, S., and Sterl, A. (2005). "A New Nonparametric method to Correct Model Data: Application to Significant Wave Height from the ERA-40 Re-Analysis." *Journal of Atmospheric and Oceanic Technology*, 22, 443-459
- Colleter, G., Cummings, P., Aguilar, P., Walters, R., and Boswood, P. "Monitoring of Tweed River entrance, dredging and nourishment activities." *Coastal and Ports Conference 2001*, 259-264.
- Cowell, P. J., Roy, P. S., and Jones, R. A. (1995). "Simulation of large-scale coastal change using a morphological behaviour model." *Marine Geology*, 126, 45-61
- D'Agata, M., and Tomlinson, R. "Discussion of the dredging of the internal delta of Currumbin estuary and its impact on adjacent beaches." *Ports and Coasts Australian Conference*.
- Dagnelie, P. (1975). "Analyse statistique a plusieurs variables." *Les Presses agronomiques de Gembloux, diffusion Vnader-Oyez.*, 362
- Delft Hydraulics Laboratory. (1970). "Gold Coast, Queensland, Australia - Coastal Erosion and Related Problems." 257, Delft Hydraulics Laboratory.
- Delft Hydraulics Laboratory. (1992). "Southern Gold Coast Littoral Sand Supply." H85, Delft Hydraulics Laboratory.
- DHL. (1992). "Southern Gold Coast Littoral Sand Supply." H85, Delft Hydraulics Laboratory.
- Goodwin, I. D., Stables, M. A., and Olley, J. M. (2006). "Wave climate, sand budget and shoreline alignment evolution of the Iluka-Woody Bay sand barrier, northern New South Wales, Australia, since 3000 yr BP." *Marine Geology*, 226, 127-144
- Kamphuis, J. W. (1991). "Alongshore Sediment Transport Rate." *Journal of Waterway, Port, Coastal, and Ocean Engineering*, 117(6), 624-640
- Kamphuis, J. W. "Alongshore transport of sand." *28th International Conference on Coastal Engineering*, Cardiff, Wales, 2478-2491.
- Patterson, D. C. "Sand Transport and Shoreline Evolution, Northern Gold Coast, Australia." *9th International Coastal Symposium*, Gold Coast, Australia, 147-151.
- Ranasinghe, R., McLoughlin, R., Short, A., and Symonds, G. (2004). "The Southern Oscillation Index, wave climate and beach rotation." *Marine Geology*, 204, 273-287
- Turner, I. L., Leyden, V. M., Cox, R. J., Jackson, A., and McGrath, J. "Physical model investigations of an artificial reef for surfing and coastal protection - Gold Coast, Queensland, Australia." *COPEDEC V*, 846-857.
- Turner, I. L., Whyte, D., Ruessink, B. G., and Ranasinghe, R. (2007). "Observations of rip spacing, persistence and mobility at a long, straight coastline." *Marine Geology*, 236, 209-221
- van Enckevoort, I. M. J., Ruessink, B. G., Coco, G., Suzuki, K., Turner, I. L., Plant, N. G., and Holman, R. A. (2004). "Observations of nearshore crescentic sandbars." *Journal of Geophysical Research*, 109(C6)
- van Rijn, L. C. (1993). *Principles of Sediment Transport in Rivers, Estuaries, and Coastal Seas*, Aqua Publications, Amsterdam.
- Wright, L. D., and Short, A. D. (1984). "Morphodynamic variability of surf zones and beaches: A synthesis." *Marine Geology*, 56, 93-118